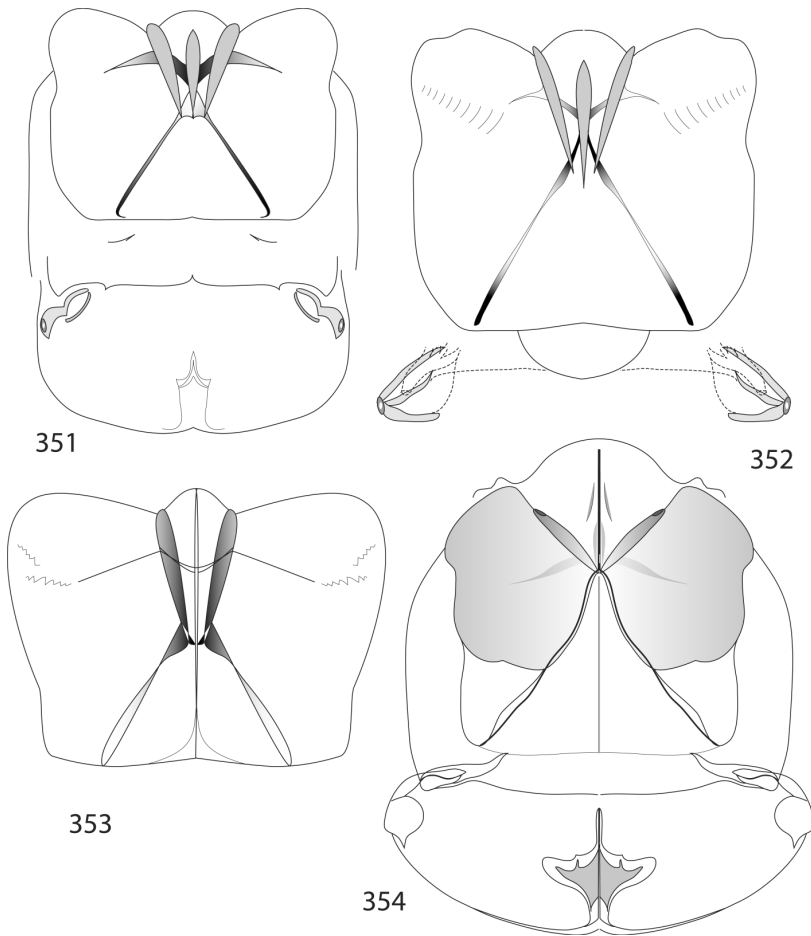Figs 347-350: Imaginal metanotum, dorsal view: *Dictyoptera aurora* (Herbst) (347); *Calochromus glaucopterus* (Guerin-Meneville) (348); *Metriorrhynchus thoracicus* (Fabricius) (349); *Plateros flavoscutellatus* Blatchley (350).

• As the regular transverse reticulation is typically associated with advanced elytral structures, such as the presence of suture flanges, it is here hypothesized to be a derived condition of the elytron.

Metathorax: The metathorax in Lycidae consists of the metanotum, metapleuron and metaventrite; the metapleuron is subdivided into the metepisternum and metepimeron. The metatrochantin, though usually regarded as a part of the pleuron, is attached to the metacoxa, and is discussed in the Leg section below.

Typically the metapleuron is not covered by the elytra and is almost completely visible externally, except at distal extremity, especially in forms where the metathorax appears laterally compressed (e.g. *Ceratoprion*, Fig. 85); but only slightly more concealed in other lycids with a more flattened metathorax, which is compressed dorsoventrally.

Figs 351-354: Imaginal metanotum, dorsal view: *Lyroneces optabilis* (Kleine) (351); *Scarelus umbrosus* Kleine (352); *Platerodrilus* sp. (353); *Calopteron reticulatum* (Fabricius) (354).

Metanotum: The metanotum is typically transverse, being conspicuously elongate in *Dexoris* (Fig. 358), slightly less so in *Ceratoprion* and *Metriorrhynchus* (Figs 349, 357). The metanotum is divided into quite a number of sclerites and bears several conspicuous sutures and sulci. Five major sclerites of the lycid metanotum are the prescutum, two parts of the divided scutum, scutellum and postnotal plate.

The relative size of the scutellum and, consequently, position of the transverse allocrista, which arises from the anterior apex of the scutellum, is variable. Its apex may lie slightly posteriad of the middle of the scutum (e.g. *Lycostomus*, Fig. 346) or just slightly posteriad of the anterior margin of the scutum (e.g. *Dictyoptera*, *Metriorrhynchus*, *Plateros*, Figs 347, 349, 350). The scutellum may be divided medially by a suture (*Calopteron*, *Platerodrilus*, *Macrolycus*, *Plateros*, *Caenia*, *Taphes*, Figs 350, 353, 354, 355, 356, 359). The allocrista never extends to lateral
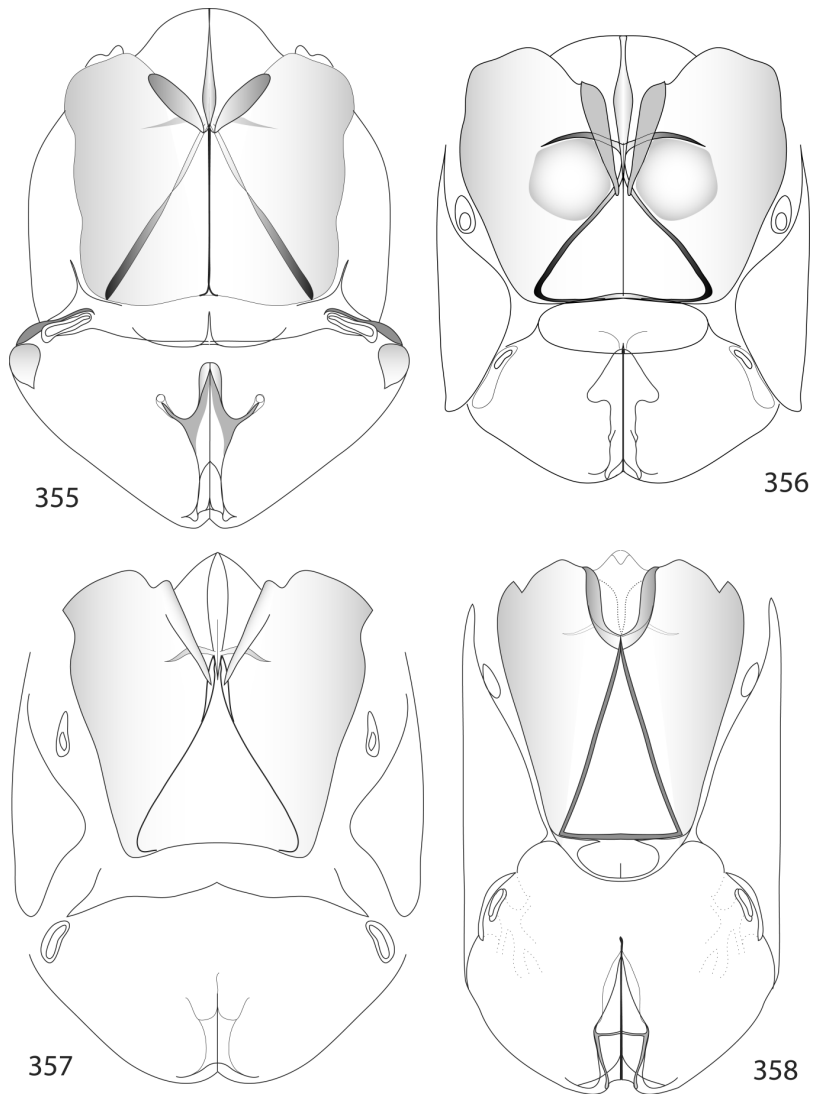
Figs 355-358: Imaginal metanotum, dorsal view: *Caenia kirschi* Bourgeois (355); *Taphes brevicollis* Waterhouse (356); *Ceratoprion* sp. (357); *Dexoris tessmani* Bocák & Bocáková (358).

margins of the scutum (e.g. Figs 346-359), varying from inconspicuous and short (e.g. *Dexoris*, *Ceratoprion*, Figs 351, 358) to conspicuous and long (e.g. *Calochromus*, Fig. 348). The relative size and location of the base of the scutoprescutal ridge also varies considerably, from inconspicuous apodemes arising from the scutellar apex (e.g. *Dexoris*, *Ceratoprion*, Figs 357, 358) to conspicuous sclerites with their bases posteriad of the middle of scutellum (e.g. *Lycostomus*, *Calochromus*, *Dictyoptera*, Figs 346, 347, 348). The postnotal plate varies from relatively small and narrow (*Dexoris*, Fig. 358) to large and broad (e.g. *Metriorrhynchus*, Fig. 349).
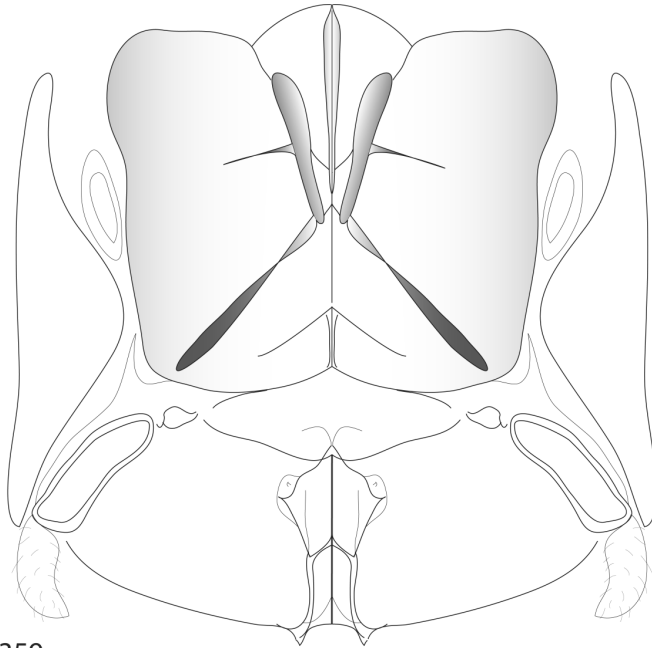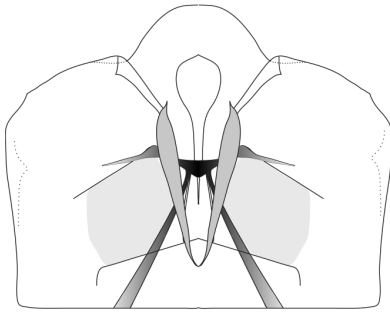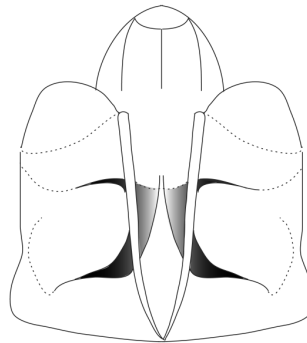
Figs 359-361: Metanotum, dorsal view: *Macrolycus flabellatus* (Motschulsky) (359); *Lampyris* sp. (360); *Cantharis fusca* Linnaeus (361).

• Plesiomorphic conditions of the metanotal structures are unknown.

Metapleuron: The metepisternum is always elongate and rigidly connected to the metepimeron, being not attached to the metaventrite (e.g. *Ceratoprion*, Fig. 224). Both the ventral and dorsal margins of the metepisternum are typically straight, the sclerite more or less conspicuously widening anteriorly (e.g. Figs 287, 295). Exceptions are *Calopteron* and *Caenia* (Figs 210, 223), with the ventral metepisternal margin convex ventrally. The subalare is separate and well noticeable in all taxa (e.g. Figs 287, 295), the basalare fused to the metepisternum.
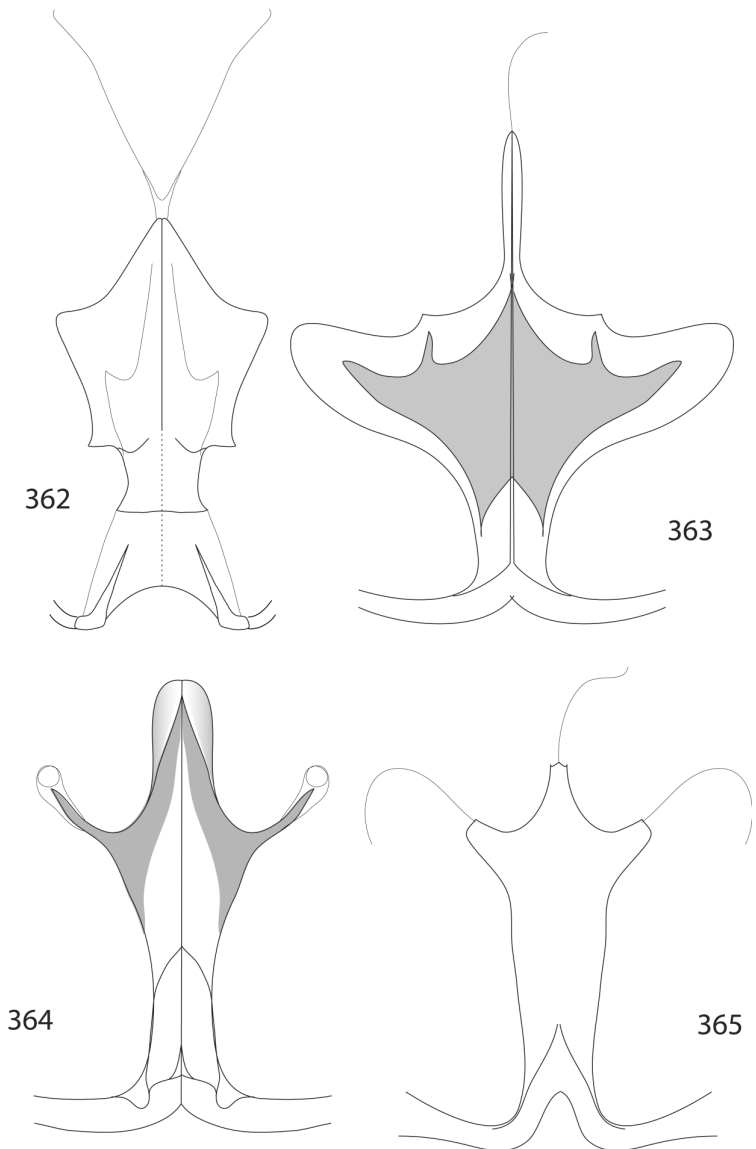
Figs 362-365: Metendosternite, dorsal view: *Lycostomus praeustus* (Fabricius) (362); *Calopteron reticulatum* (Fabricius) (363); *Caenia kirschi* Bourgeois (364); *Lycinella parvula* Gorham (365).

Metaventrite: The metaventrite (the true metasternum being also totally invaginated, forming the endosternites and represented on the surface only as the median groove, or the discrimen - Campau, 1940; Ferris, 1940, Beutel & Hass, 2000, Lawrence, 1999) is typically subquadrate or transverse (e.g. Figs 207, 210, 225, etc.), sometimes being conspicuously elongate (*Lyroneces*, *Dexoris*, *Ceratoprion*, *Caenia*, *Lycinella*, Figs 209, 215, 218, 223, 224). It is not rigidly attached to the
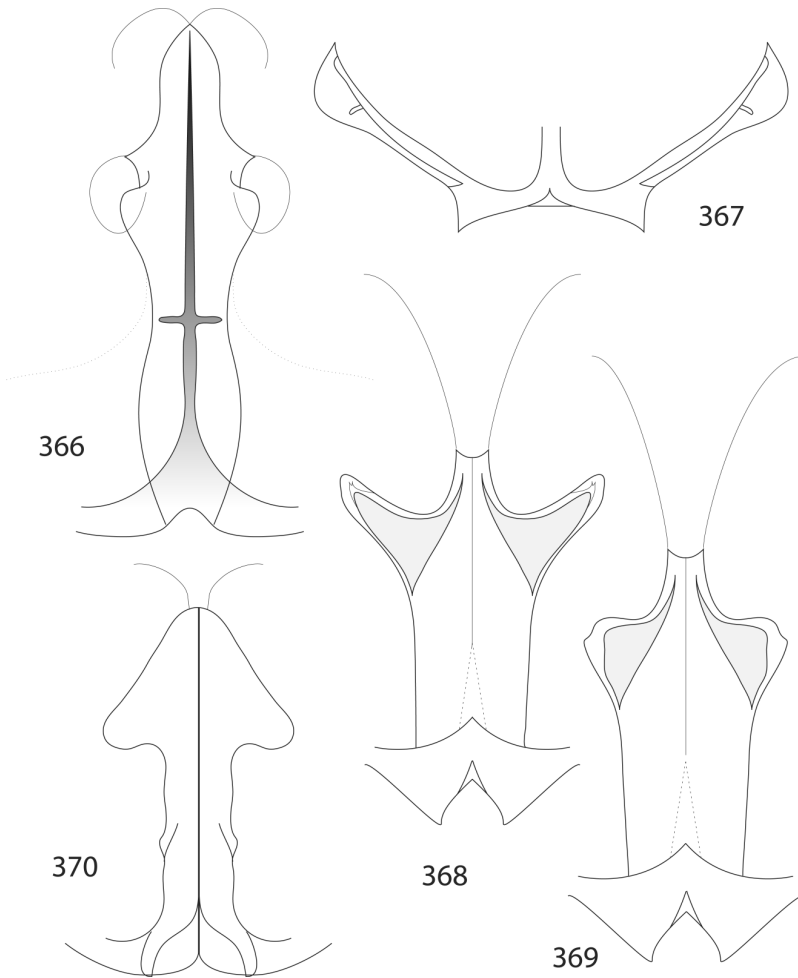
Figs 366-370: Metendosternite, dorsal view: *Helcophorus miniatus* Fairmaire, male (366); *Helcophorus miniatus* Fairmaire, female (367); *Dictyoptera aurora* (Herbst), male (368); *Dictyoptera aurora* (Herbst), female (369); *Taphes brevicollis* Waterhouse (370).

metepisternum, the dehiscence is always more or less manifest, reaching its greatest degree in *Ceratoprion* (Fig. 224); the posterolateral angles sometimes are little projected to meet the metacoxa-metapleuron articulation (*Lyroneces*, *Dexoris*, *Caenia*, *Ceratoprion, Helcophorus*, Figs 209, 212, 215, 223, 224, also *Thilmanus*, Fig. 226). The metaventrite is always slightly emarginate between the coxae (Figs 207-225), but never receives the anterior median process of the first ventrite, which is absent, with the only exception found in *Calochromus*, where it is only feebly manifest. The lateral margin of the lycid metaventrite is more or less straight or slightly convex (Figs 207-225), while that in *Cantharis* is conspicuously concave (Fig. 230).

The metasternal suture, or the discrimen, is complete, reaching the mesoventrite in *Lycostomus*, *Lyroneces*, *Calopteron*, *Ceratoprion* and *Dexoris* (Figs 207, 209,
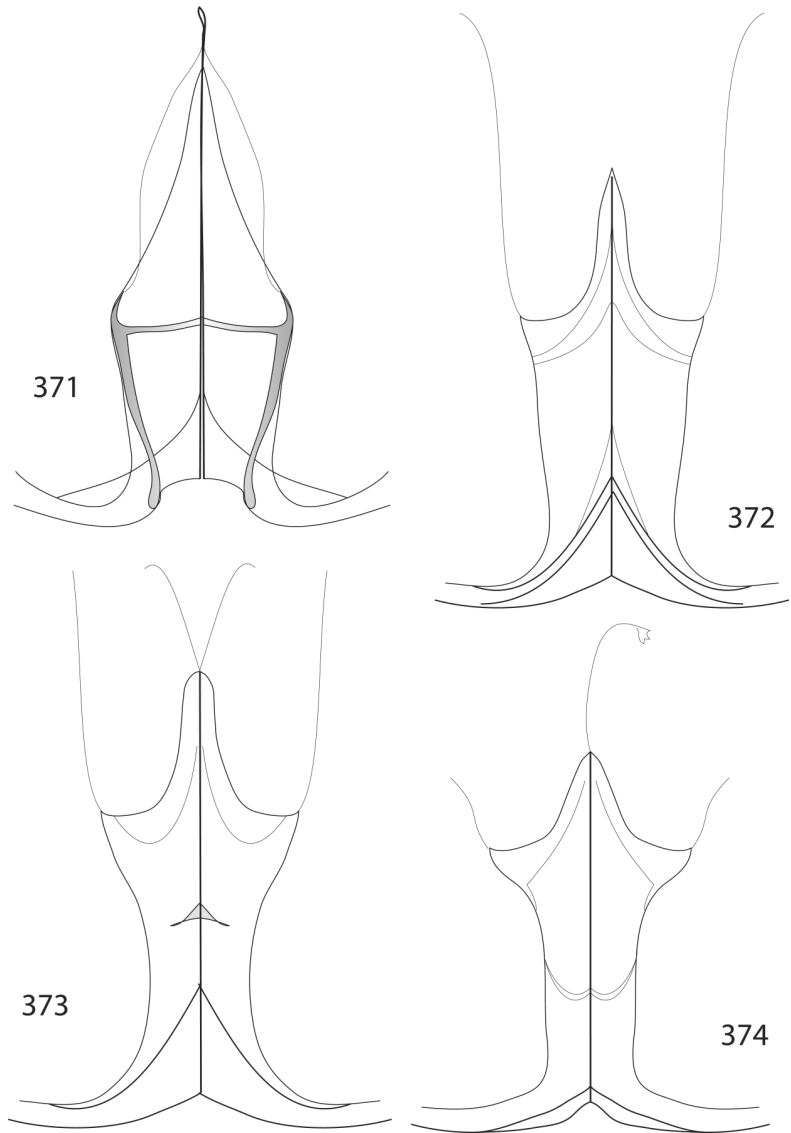
Figs 371-374: Metendosternite, dorsal view: *Dexoris tessmani* Bocák & Bocáková (371); *Lyroneces optabilis* (Kleine) (372); *Scarelus umbrosus* Kleine (373); *Platerodrilus* sp. (374).

210, 215, 224). The rest of the studied lycid taxa (e.g. Figs 208, 220, 223, 225, etc.), as well as *Thilmanus*, *Lampyris*, *Cantharis* and *Phengodes* (Figs 226, 227, 229, 230) have short to long metasternal suture that does not reach the mesosternal posterior margin. It is noteworthy that none of the taxa with the divided mesonotum (*Caenia*, *Metriorrhynchus*, and *Thilmanus*, Figs 217, 223, 226) has a complete metasternal suture, which may signify that the mesosternal and metasternal sutures are not homologous. Complete disappearance of the hind wing in female of
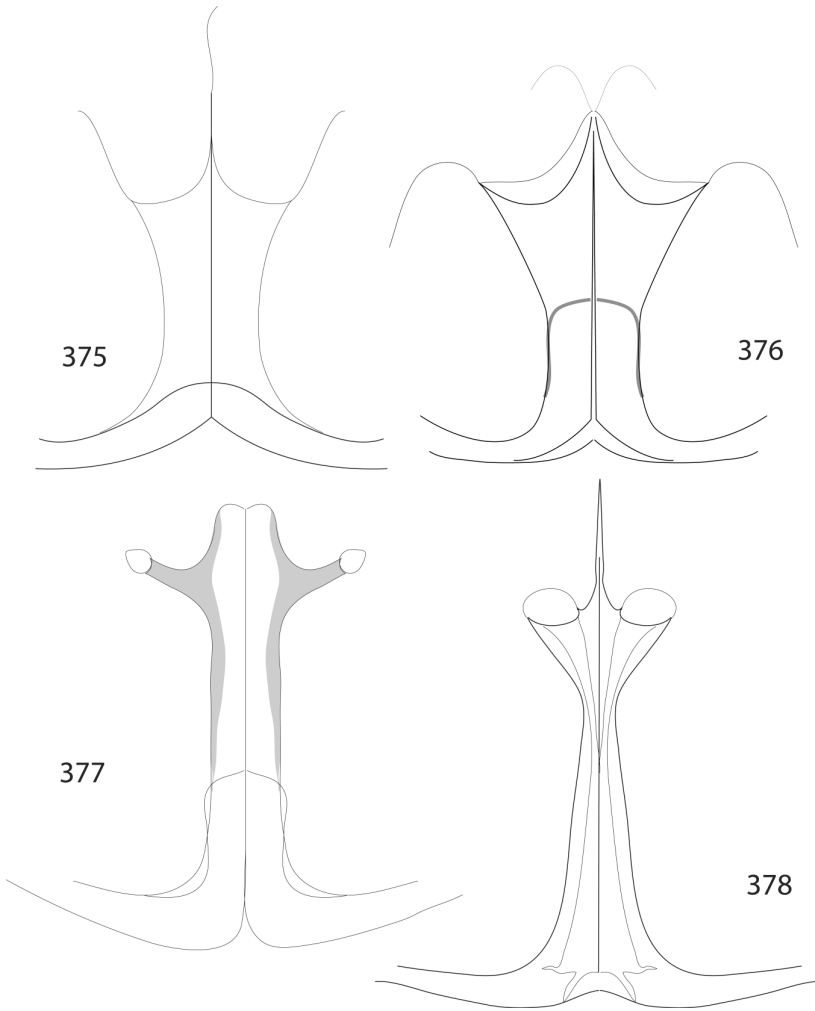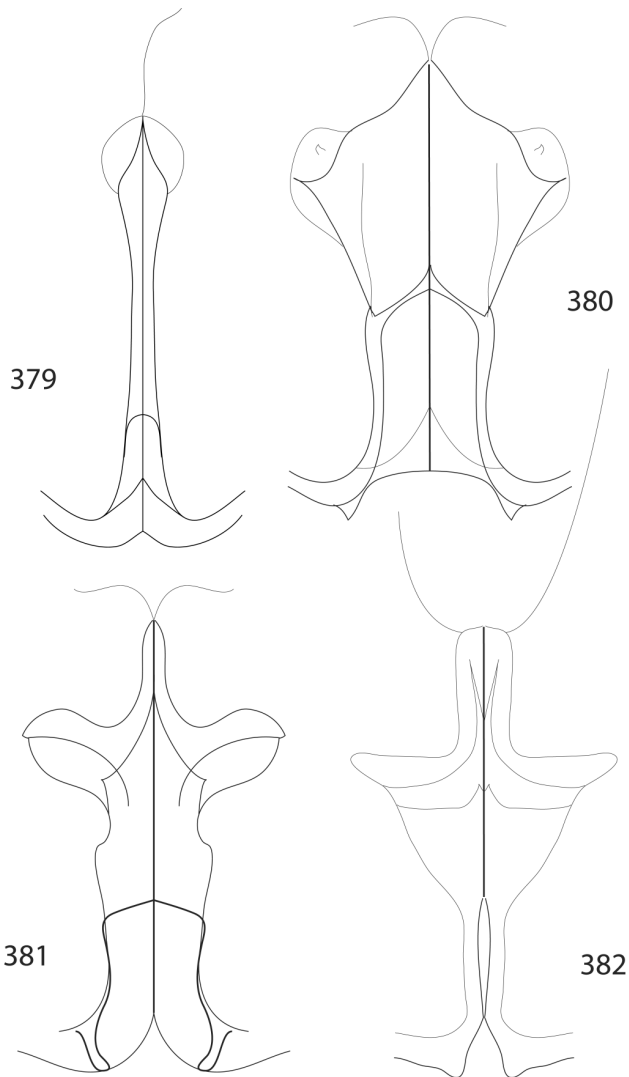
Figs 375-378: Metendosternite, dorsal view: *Ceratoprion* sp. (375); *Aferos* sp. (376); *Plateros flavoscutellatus* Blatchley (377); *Metriorrhynchus thoracicus* (Fabricius) (378).

Helcophorus miniatus does not affect the length of its metaventrite, but its metasternal suture forks anteriad of the middle of the sclerite (Fig. 212).

• The broadly separated metaventrite and metapleuron with the posterolateral angles of the metaventrite feebly projected to meet the metacoxa-metapleuron articulation is deemed primitive.

• The absence of anterior median process of the first ventrite, and, consequently, minimal coadaptation between the metaventrite and the abdomen, is considered plesiomorphic.

• Plesiomorphic condition of the metasternal suture (dividing the sclerite into two parts or incomplete) is unclear.

Figs 379-382: Metendosternite, dorsal view: *Mesolycus shelfordi* (Bourgeois) (379); *Macrolycus flabellatus* (Motschulsky) (380); *Conderis signicollis* (Kirsch) (381); *Calochromus glaucopterus* (Guerin-Meneville) (382).

Metendosternite: The structure of metendosternite is diverse in the family, with the simplest structures found in *Lycinella* and *Ceratoprion* (Figs 365, 375) as well as in *Thilmanus* (Fig. 385), where the transverse suture typically present in a lycid metendosternite is absent. The transverse suture seems to be vestigial also in *Lyroneces*, *Taphes* and *Scarelus* (Figs 370, 372, 373). *Mesolycus* and *Dexoris* (Figs 371, 379) have another version of a simplified metendosternite: they do have the transverse suture, but the lateral arms are absent. The relative size of the metendosternite varies considerably from very inconspicuous compared to the size
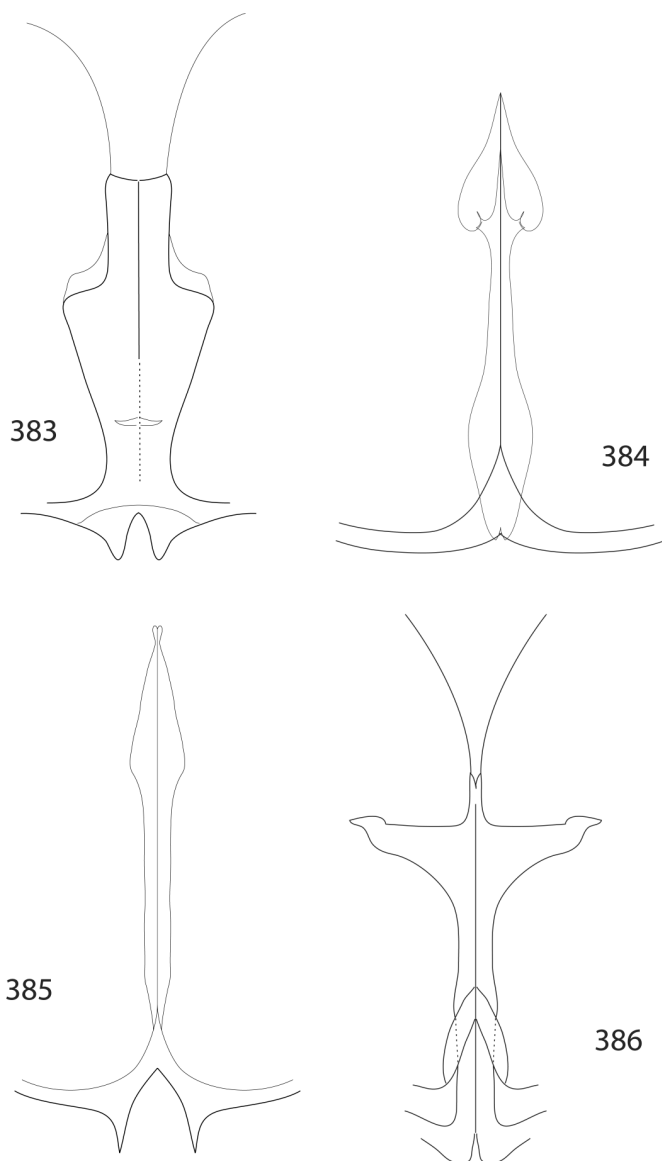
Figs 383-386: Metendosternite, dorsal view: *Lampyris* sp. (383); *Phengodes* sp. (384); *Thilmanus obscurus* (Baudi) (385); *Cantharis fusca* Linnaeus (386).

of the metathorax (e.g. *Ceratoprion*, *Dexoris*, Figs 357, 358) to large, reaching the posterior margin of the postnotal plate (e.g. *Taphes*, *Macrolycus*, Figs 356, 359) or of the metascutellum (e.g. *Thilmanus*). None of the structures of the studied taxa, however, are comparable in size with the metendosternite of *Tenomerga* (Fig. 233), which almost attains to the mesothorax.
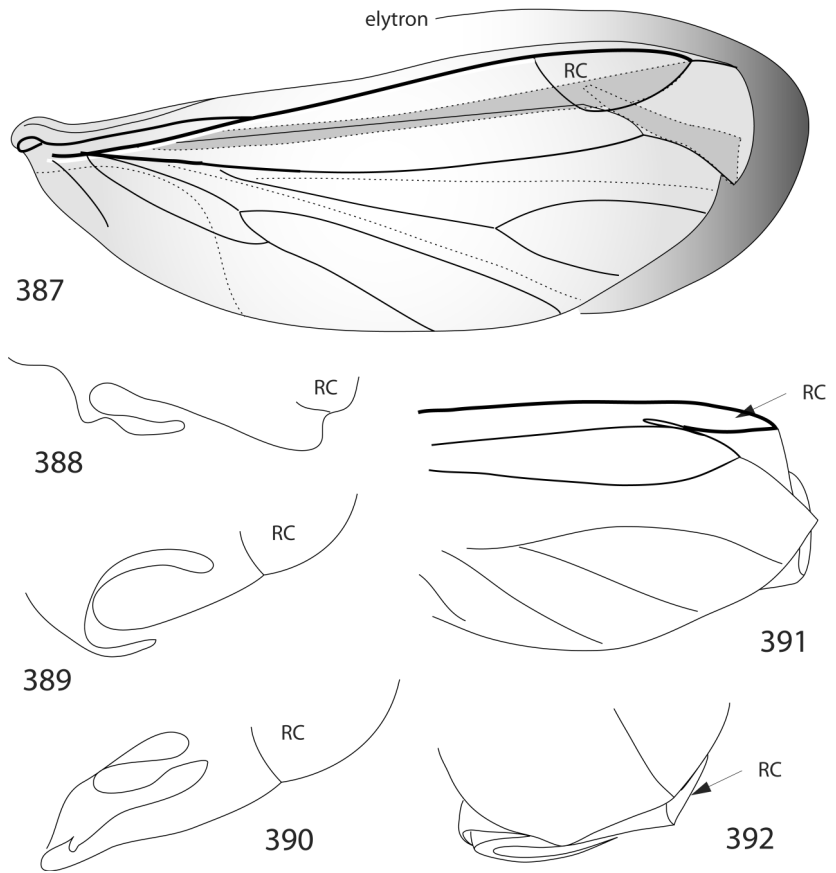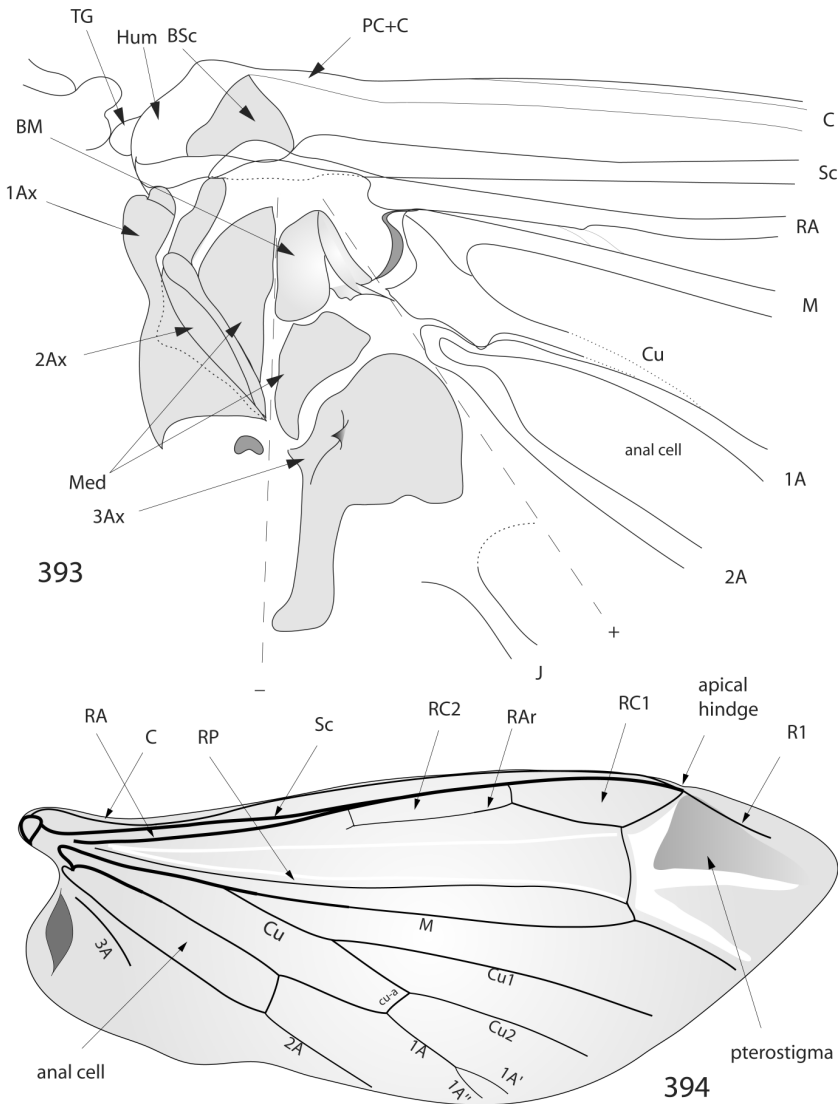
Figs 387-392: Metathoracic wing structures: *Lyroneces optabilis* (Kleine), folded wing, ventral view (387); same, folded apical field, apical view (388); *Lygistopterus laetus* Gorham, folded apical field, apical view (389); *Lychnuris* sp., folded apical field, apical view (390); *Cantharis fusca* Linnaeus, folded wing, apical portion, ventral view (391), same, folded apical field, apical view (392).

RC - radial cell.

The apical portion of metendosternite is typically not emarginate (e.g. *Helcophorus*, Figs 366) or only slightly emarginate (in *Dictyoptera*, Fig. 368). The anterior tendons are usually approximate basally (e.g. *Lycostomus*, *Scarelus*, Figs 363, 373). The metendosternal ventrolateral processes are absent.

Quite striking is the dissimilarity of the male and female metendosternites of *Helcophorus miniatus* (Figs 366, 367), the female of which is apterous. The female metendosternite consists of a pair of widely separated transverse bars, comparable to the mesendosternite and to the larval condition (Crowson, 1981), and resembles none of those of other lycids or cantharoids, the difference between the sexes of one species exceeding the difference between almost any, even totally unrelated, coleopteran families (Crowson, 1938). There seem to be the following possible explanations of this phenomenon:

Figs 393-394: Metathoracic wing structures: *Lycostomus praeustus (Fabricius*, wing base, dorsal view (393); *Lycostomus similis* (Hope), wing, dorsal view (394).

Ax - axillary sclerite; BM - median basivenale; BSc - subcostal basivenale; Hum - humeral plate; Med - medial plate; RC - radial cell; TG - tegula.

a) the metendosternite of Coleoptera is subject to fast and fundamental modifications correlated with the degree of development of metathoracic wings and is of little practical use for taxonomic purposes (this contradicts to what is known of the thorax morphology of various beetles and other hexapod groups - Crowson, 1938; 1981; Snodgrass, 1935; as well as to Dollo's law);
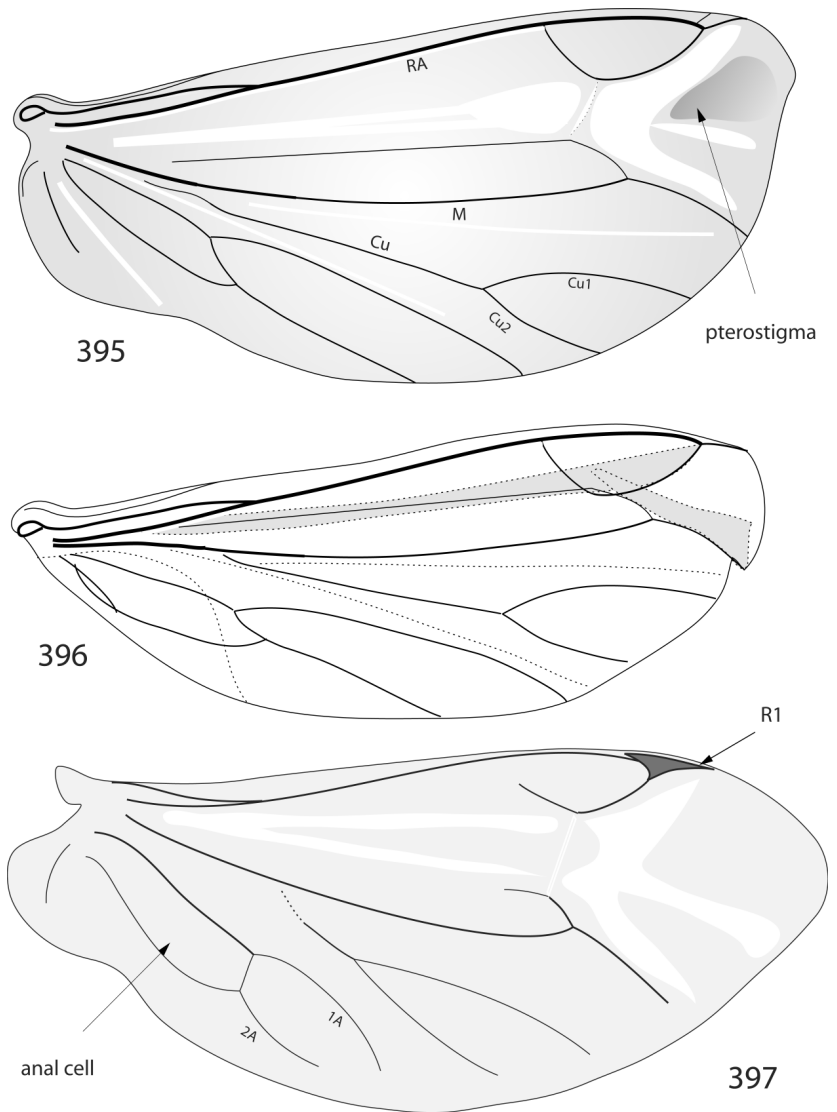
Figs 395-397: Metathoracic wing, dorsal view: *Lyroneces optabilis* (Kleine), unfolded wing (395); same, folded wing (396); *Ceratoprion* sp., unfolded wing (397).

b) the female has never had fully developed metathoracic wings (this hypothesis seems doubtful, as this case would probably have excluded development of a normal elytron and other typical pterothoracic structures);

c) the female started to loose its metathoracic wings prior to emergence of most of the Recent beetles families and its metendosternite underwent significant reverse changes at a normal evolution process speed, comparable to that of other Coleoptera, while the male hind wing structures remained unchanged (this
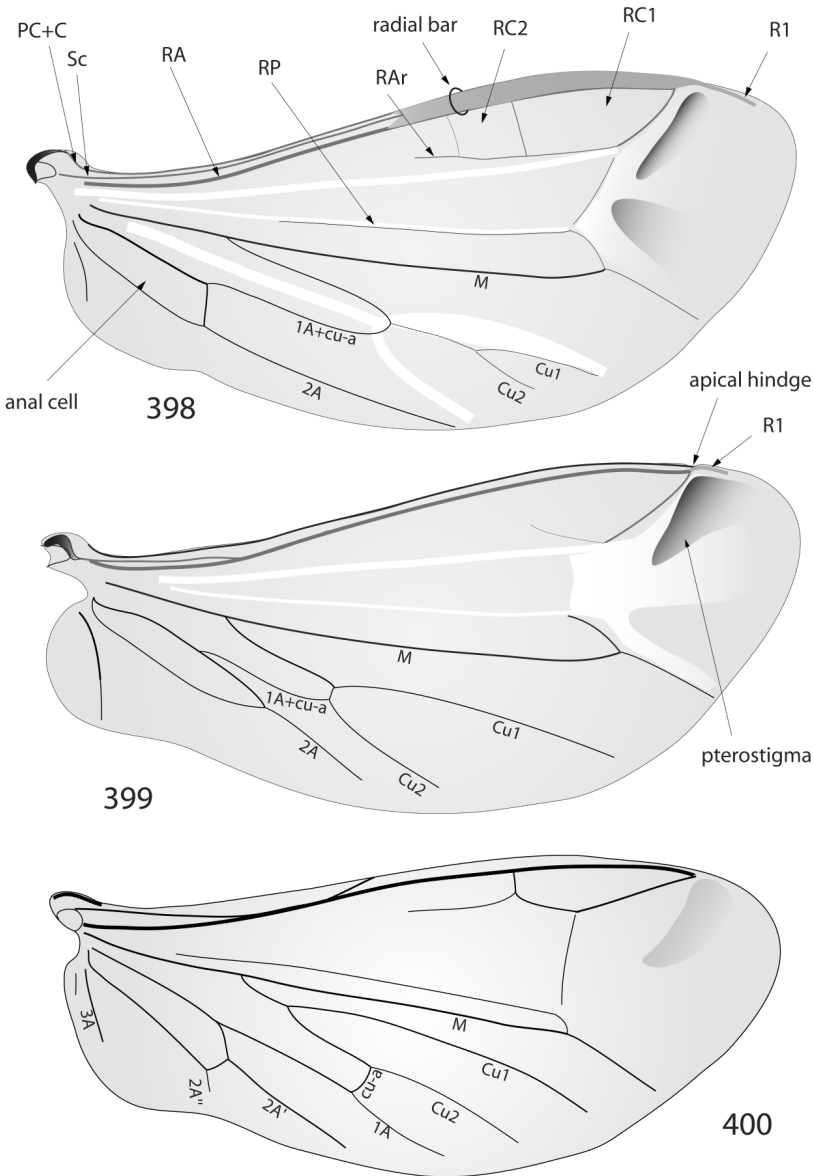
Figs 398-400: Metathoracic wing, dorsal view: *Dexoris tessmani* Bocák & Bocáková (398); *Mimolibnetis apicalis* Pic (399); *Scarelus umbrosus* Kleine (400).

hypothesis seems to be contradicting both to Dollo's law, with the metendosternal structures regaining its lost characters, and to the conventional timing of origin of the Lycidae); and

d) the female metathoracic wings started to develop much later than the male ones and were then, at a point when the metendosternite was still in the ancestral condition, gradually reduced (this hypothesis seems to be less contradicting to the
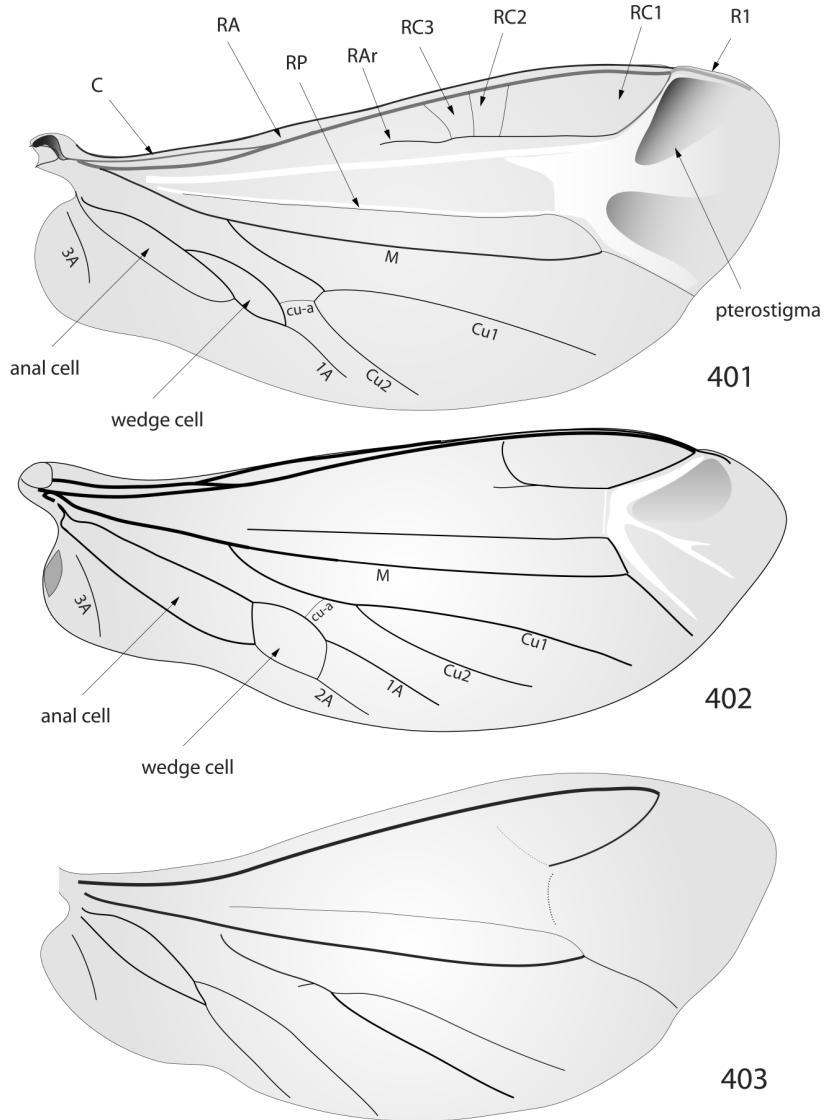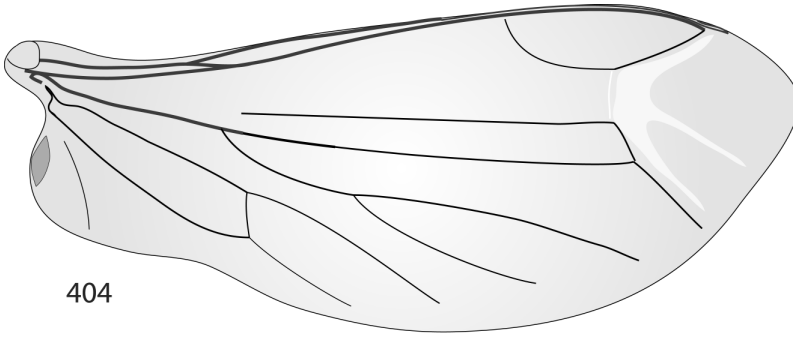
Figs 401-403: Metathoracic wing, dorsal view: *Lampyrolycus bicolor* Kazantsev (401); *Dilophotes depressicornis* Pic (402); *Platerodrilus* sp. (403).
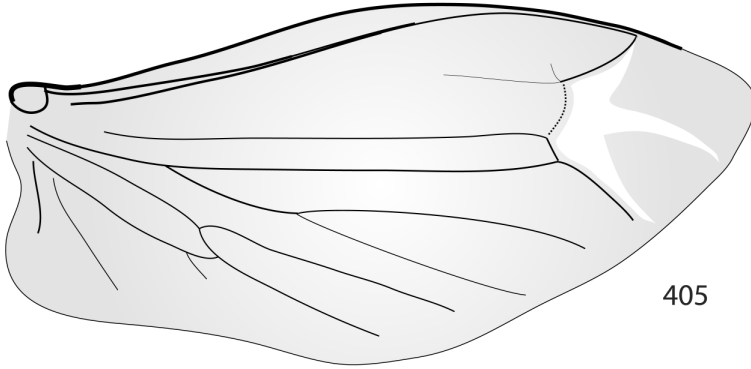
RC - radial cell.

general pterygote morphology data, disputing the phylogenetic aspects of neoteny in the Lycidae).
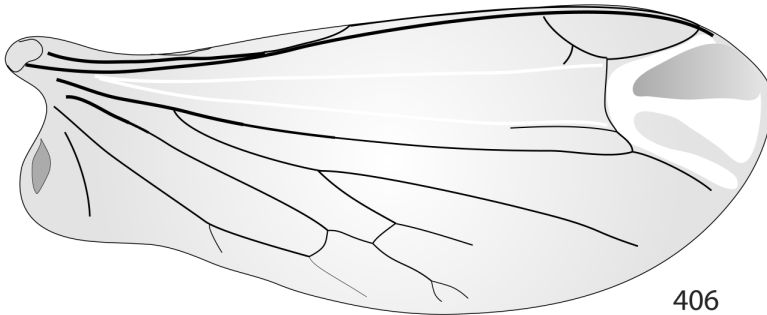
The c) and d) options may be connected with possible relatively recent occurrence of the paedomorphosis/neoteny in *H. miniatus*. All options were taken into consideration for a further analysis (in the Biology and Phylogeny sections below).
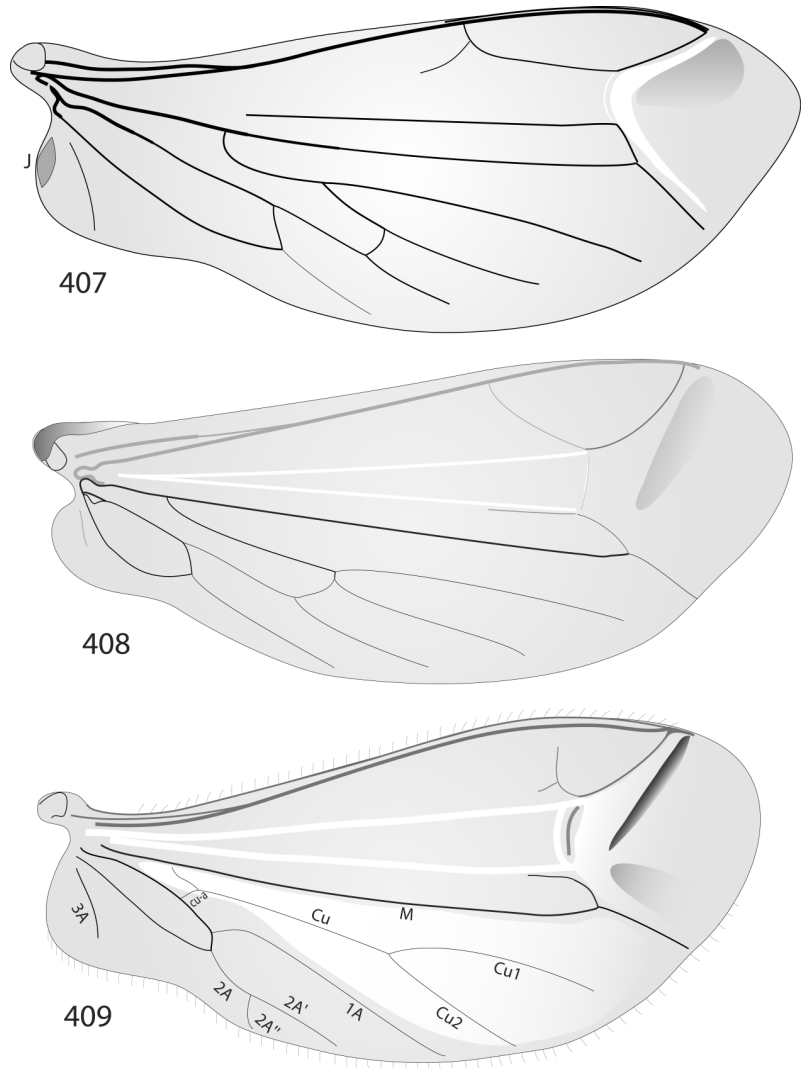
Figs 404-406: Metathoracic wing, dorsal view: *Mesolycus shelfordi* (Bourgeois) (404); *Macrolycus flabellatus* (Motschulsky) (405); *Conderis signicollis* (Kirsch) (406).

In contrast to the extremely variable metendosternite of the Lycidae the same structure of the Cantharidae demonstrates remarkable similarity to the *Cantharis* type (Fig. 386), even in lineages otherwise very different morphologically, such as Malthininae, Silinae, Chauliognathinae (Brancucci, 1980). The *Phengodes* metendosternite is also close to this type (Fig. 384).

• The larval condition, i.e. the metendosternite consisting of a pair of transverse bars, is deemed primitive.

• The absence of the metendosternal transverse suture and lateral arms is considered plesiomorphic.
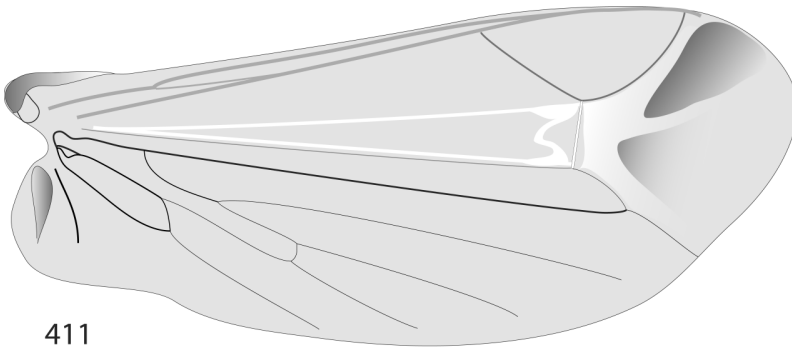
Figs 407-409: Metathoracic wing, dorsal view: *Caenia kirschi* Bourgeois (407); *Lycinella parvula* Gorham (408); *Miniduliticola nelsoni* Kazantsev (409).

• The small size of the metendosternite in relation to other metathoracic structures is considered plesiomorphic.

Thoracic spiracles: The anterior (mesothoracic) spiracles are typically located anteriad of the mesothorax; they are sclerotized and completely exposed (Figs 207-225). The posterior (metathoracic) spiracles are well-developed, but typically feebly sclerotized, except that they usually have peritremes (e.g. *Calopteron*, Fig. 210); they are exposed laterally and closed ventrally by the mesepimeron. The orifice of the mesothoracic spiracles of *Macrolycus*, *Mesolycus*, *Conderis* and *Metriorrhynchus*,
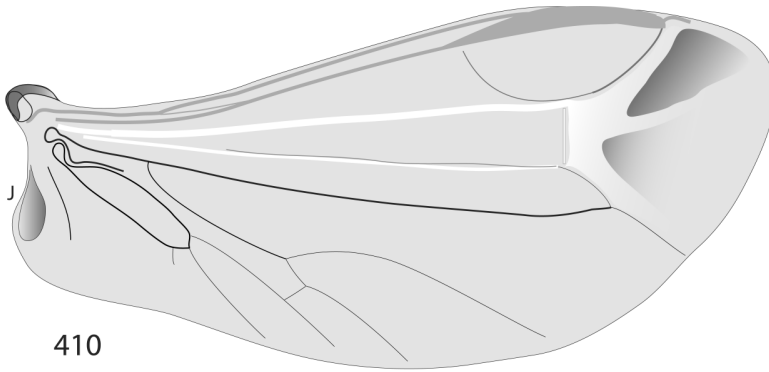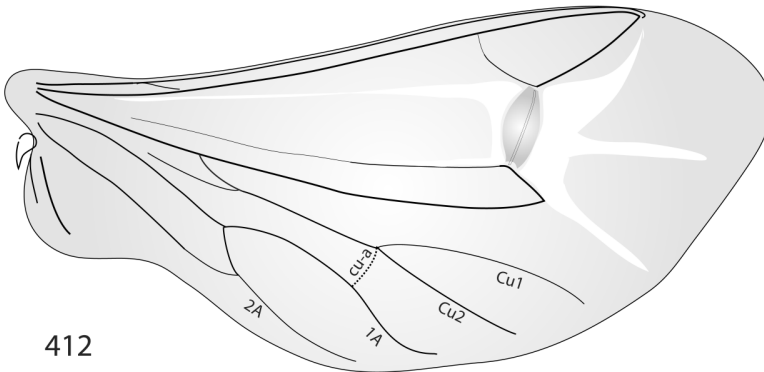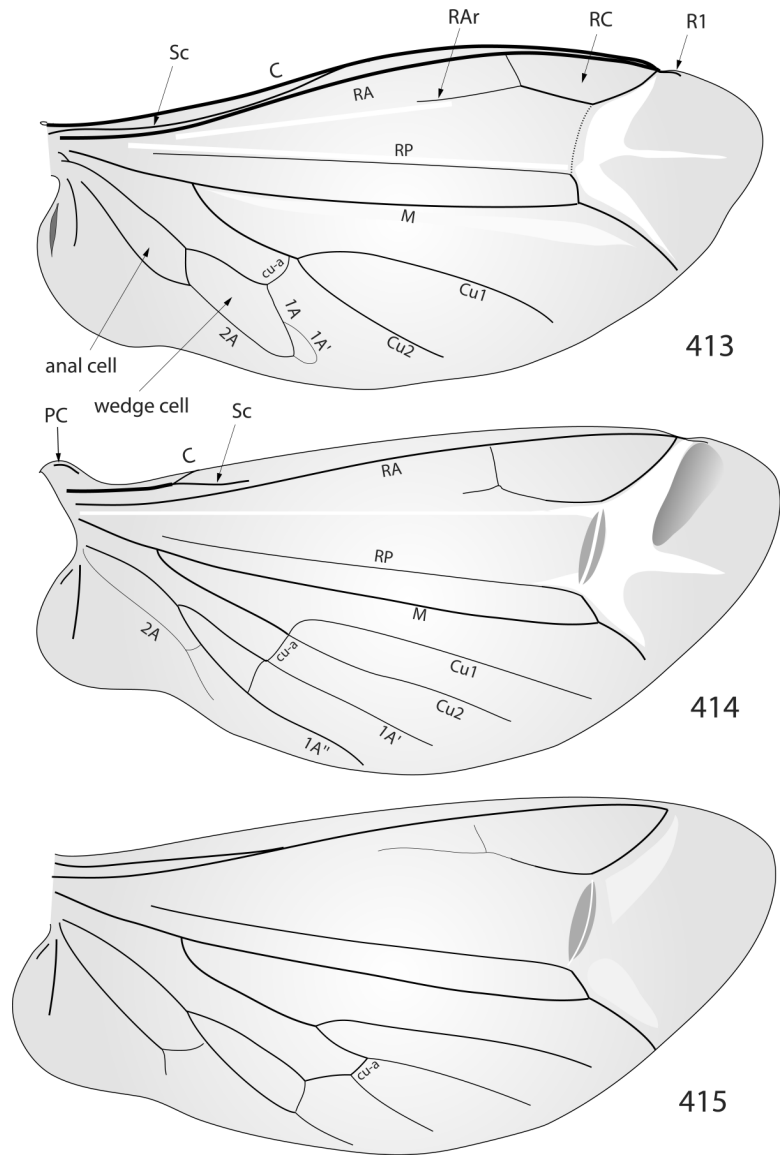
Figs 410-412: Metathoracic wing, dorsal view: *Plateros flavoscutellatus* Blatchley (410); *Metriorrhynchus thoracicus* (Fabricius) (411); *Autaphes australis* Kazantsev (412).

as well as *Broxylus*, unlike in other lycids, is hooded dorsally (Figs 217, 220, 221, 222).

The large spiracle located posterolaterally in the metathorax and usually referred to as abdominal spiracle 1, structurally resembles thoracic spiracles and has conspicuous peritremes (e.g. *Lycostomus*, *Macrolycus*, *Plateros*, Figs 346, 350, 359), being always different from the small and lacking peritremes abdominal spiracles 2-8. Almost exactly the same position of the second metathoracic spiracle

Figs 413-415: Metathoracic wing, dorsal view: *Proteros sempiternus* Kazantsev (413); *Eropterus arculus* Green (414); *Flagrax auberti* (Bourgeois) (415).

is found in *Heterojapyx* (Diplura) (Snodgrass, 1935), which has two pairs of spiracles on each of the meso- and metathorax. It also corresponds to the usual position of thoracic spiracles in Chilopoda (Snodgrass, 1935).

Metathoracic wing: The hind wings are usually well developed in both sexes, with few exceptions when the female wings are completely or partially reduced. Interestingly, when the wings are reduced partially (as in *Lycostomus sanguineus*
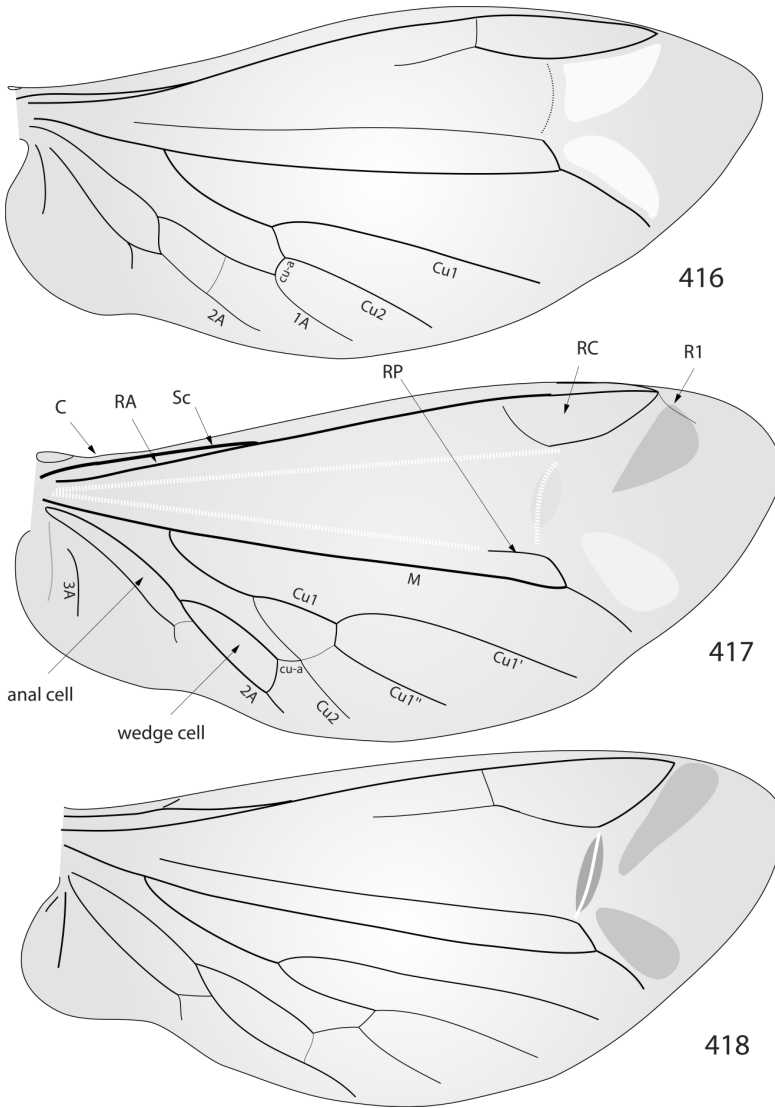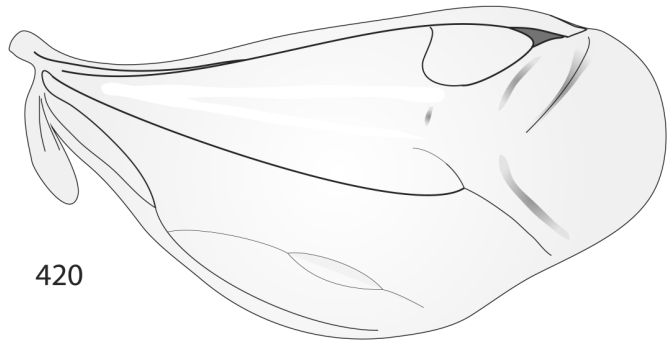
Figs 416-418: Metathoracic wing, dorsal view: *Eros humeralis* (Fabricius) (416); *Platycis minuta* (Fabricius) (417); *Aferos* sp. (418).

Gorham or *Metriorrhynchus apterous* Lea) the elytra are correspondingly reduced, and when they are reduced completely (in *Helcophorus miniatus*) the elytra are as long and as well developed as in the winged males. Typically the hind wing is completely hidden by the elytron, except in *Leptolycus heterocornis* Leng & Mutchler and *Alyculus*. In the former the wings are normally folded, while in the latter the hind wings do not fold; in both cases they considerably surpass the length of the elytra and the abdomen.
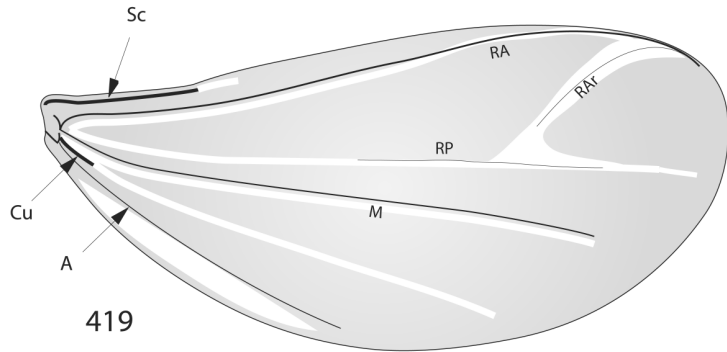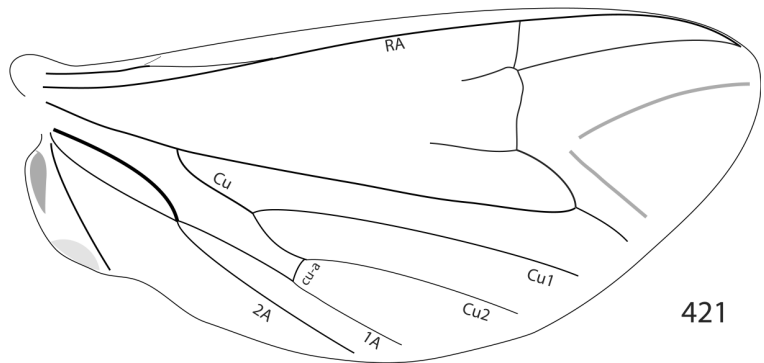
Figs 419-421: Metathoracic wing, dorsal view: *Alyculus kurbatovi* Kazantsev (419); *Thilmanus obscurus* (Baudi) (420); *Phengodes* sp. (421).

The folding system of the hind wing in Lycidae is similar to «*Cantharis*» type, but differs by a significantly lesser degree of wing reduction and a different structure of folding of the apical field. In *Cantharis* the apical field is folded both transversely and longitudinally, with two longitudinal folds underlying the radial cell, which, in its turn, underlies the medial hook (Figs 391-392), whereas in the Lycidae the apical field is folded longitudinally, with a single posterior fold slightly overhanging the posterior margin or slightly curved ventrally, the radial cell and the medial hook
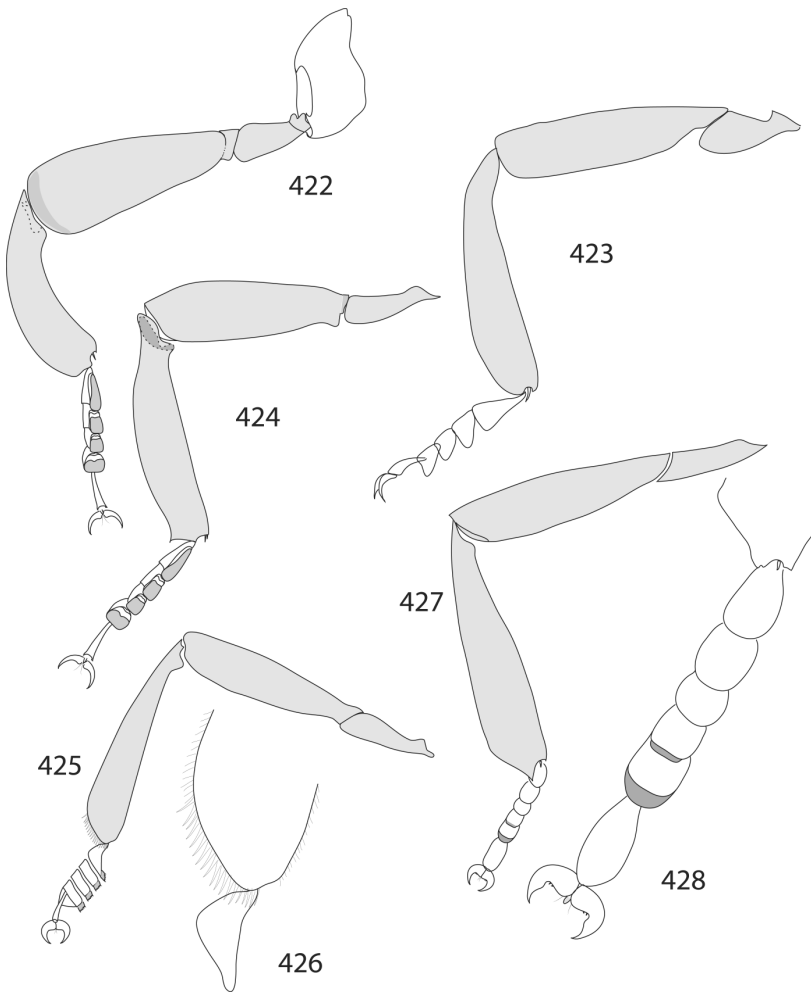
Figs 422-428: Imaginal mesothoracic leg: *Lycostomus praeustus* (Fabricius) (422); *Dictyoptera aurora* (Herbst) (423); *Calochromus glaucopterus* (Guerin-Meneville) (424); *Scarelus umbrosus* Kleine (425); same, tibial apex and tarsomere 1 (426); *Lyroneces optabilis* (Kleine) (427); same, tarsus (428).

approximated, but not underlying each other (e.g. *Lyroneces*, Figs 387-388). A slightly more derived type, represented in such taxa, as *Lygistopterus*, *Platerodrilus*, *Lampyrolycus*, etc., is characterized by the apical part folded first posteriorly and then conspicuously folded anteriorly (Fig. 389). It is noteworthy that in Cantharidae other than *Cantharis* the wing folding may be different, but is never as simple as in the Lycidae. In Lampyridae there are several types of wing folding, from the derived lycid type at the simplest end of the gradient; perhaps the most widespread in the family is the double anterior fold (Fig. 390). Only inconspicuously longitudinally folded wings occur in *Phengodes*, and this is reflected in its wing venation (Fig. 421).
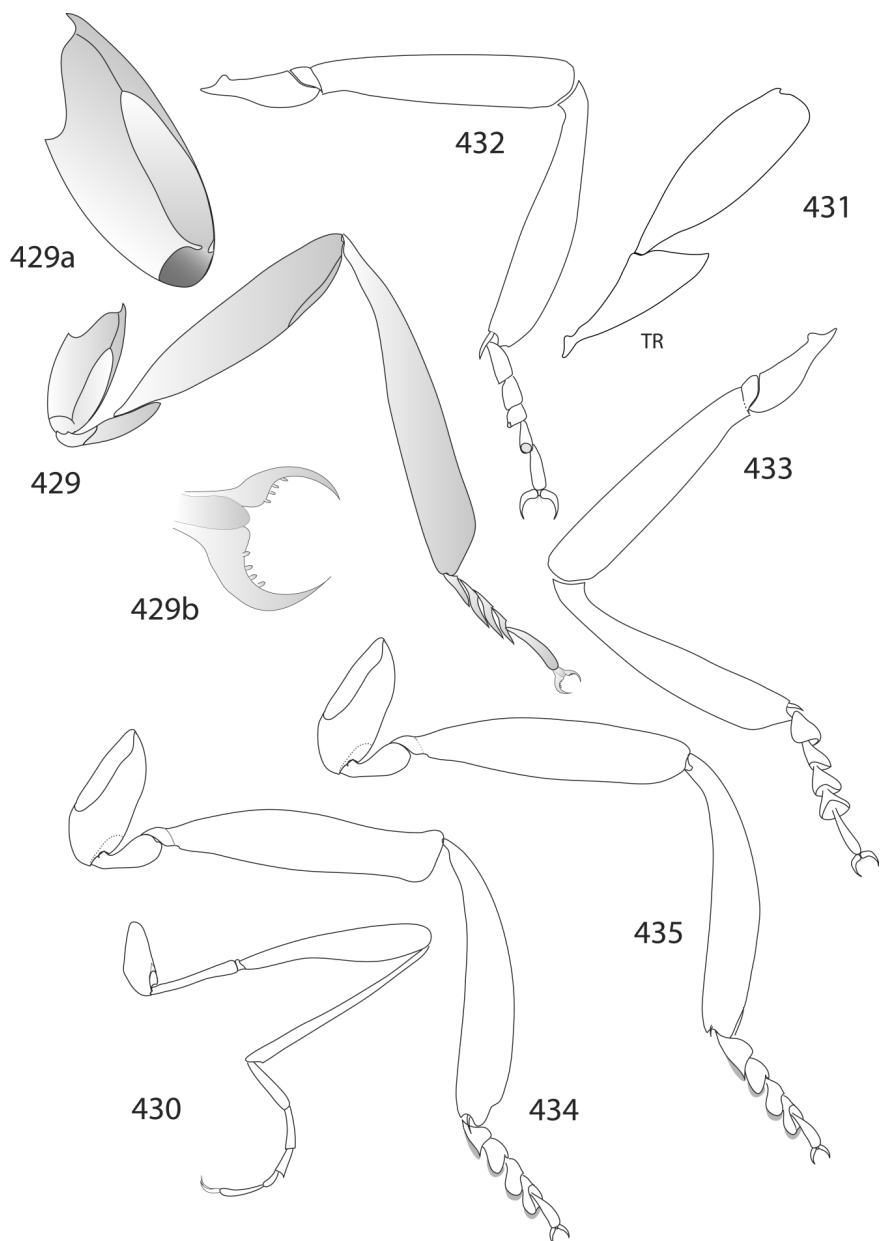
Figs 429-435: Imaginal leg structures: *Dexoris tessmani* Bocák & Bocáková, mesothoracic leg (429); same, coxa (429a); same, claws (429b); *Leptolycus heterocornis* Leng & Mutchler, mesothoracic leg (430); *Punicealis munda* (Barovskij), metathoracic trochanter and femur (431); *Platerodrilus* sp., mesothoracic leg (432); *Calopteron reticulatum* (Fabricius), mesothoracic leg (433); *Plateros flavoscutellatus* Blatchley, mesothoracic leg (434); *Metriorrhynchus thoracicus* (Fabricius), mesothoracic leg (435).

TR - trochanter.
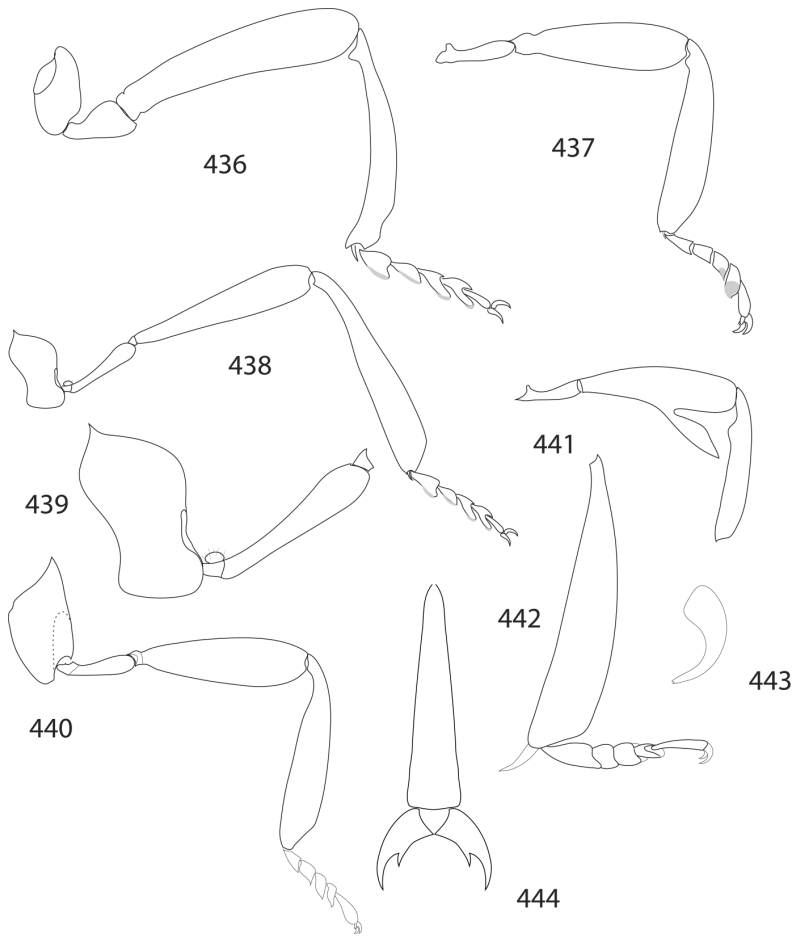
Figs 436-444: Imaginal mesothoracic leg: *Aferos* sp. (436); *Taphes brevicollis* Waterhouse (437); *Caenia kirschi* Bourgeois (438); same, coxa and trochanter (439); *Ceratoprion* sp. (440); *Cavoplateros spinipes* Pic, after Bocáková, 2001 (441); *Calcaeron sundaicus* Kazantsev (442); same, claw (443); *Dilophotes depressicornis* Pic, tarsomere 5 with claws (444).

The «*Cantharis*» type is considered the simplest and primary type in the Coleoptera (Hammond, 1979). It appears that the lycid type is yet simpler and yet more primitive. It allows reducing both the breadth and length of the wing by relaxation into several longitudinal folds. The degree of the wing reduction in lycids that use simple spring mechanism when muscles at the base of the wing are relaxed, is sometimes as low as 5 % (e.g. *Lyroneces*, Figs 395-396) and does not exceed ca. 10-15 % (compared to 25 % in Cupedidae, up to 50 % in Adephaga and up to 80 % in Staphylinoidea where other types of mechanisms are employed). This type of wing-folding mechanism does not use structures external to the wing (Hammond, 1979). As a matter of fact, the wing folding in some of the Lycidae is so insignificant that the elytron is longer than even the fully spread hind wing (e.g. *Lyroneces*, Figs 387, 395, 396).
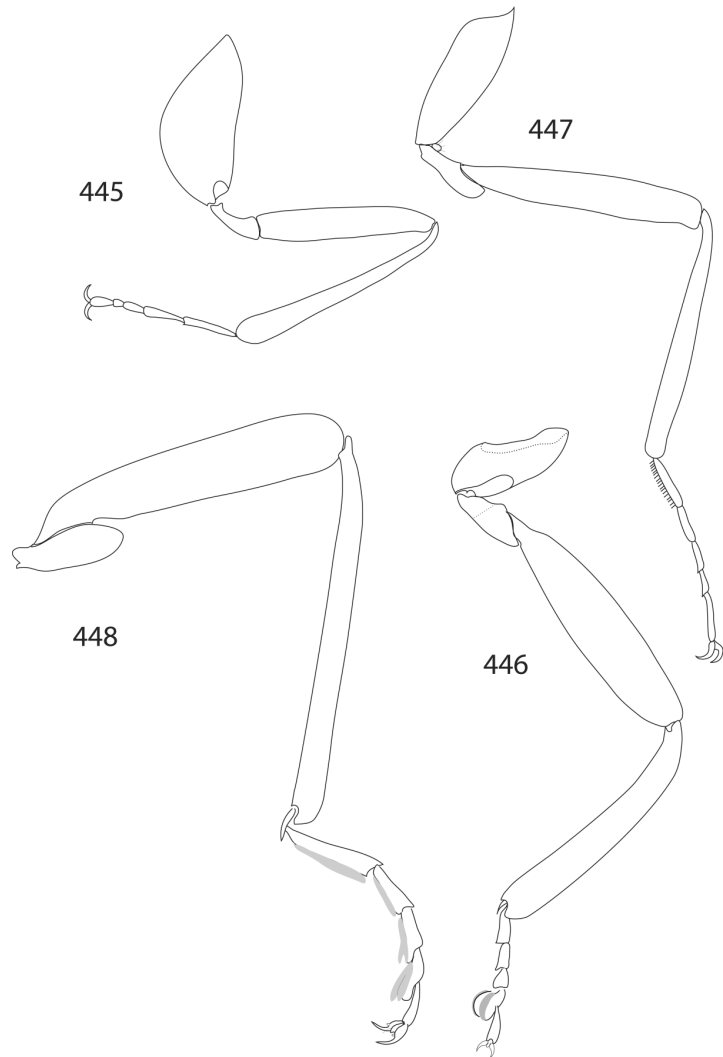
Figs 445-448: Imaginal mesothoracic leg: *Thilmanus obscurus* (Baudi) (445); *Lampyris* sp. (446); *Phengodes* sp. (447); *Cantharis fusca* Linnaeus (448).

The pterostigma in Lycidae is located distad of, but not in the radial cell (e.g. *Lycostomus*, *Lyroneces*, *Mimolibnetis*, Figs 394, 395, 399), and the radial hinge is absent. Hence, the lycid radial cell is probably not homologous with the radial cell of Archostemata, which has the pterostigma inside (Kukalova-Peck & Lawrence, 1993). In both cases, however, the pterostigma is in the center of the anterior part of the radial fold, which suggests that the Archostematan radial cell and the lycid (and Polyphagan) pterostigma may prove to be homologous areas of the wing.

The fluting typically is uniformly convex, with only M, except at its very base, Sc and J veins concave. In *Miniduliticola*, however, the M and Sc veins in their proximal half are convex as well (Fig. 409).
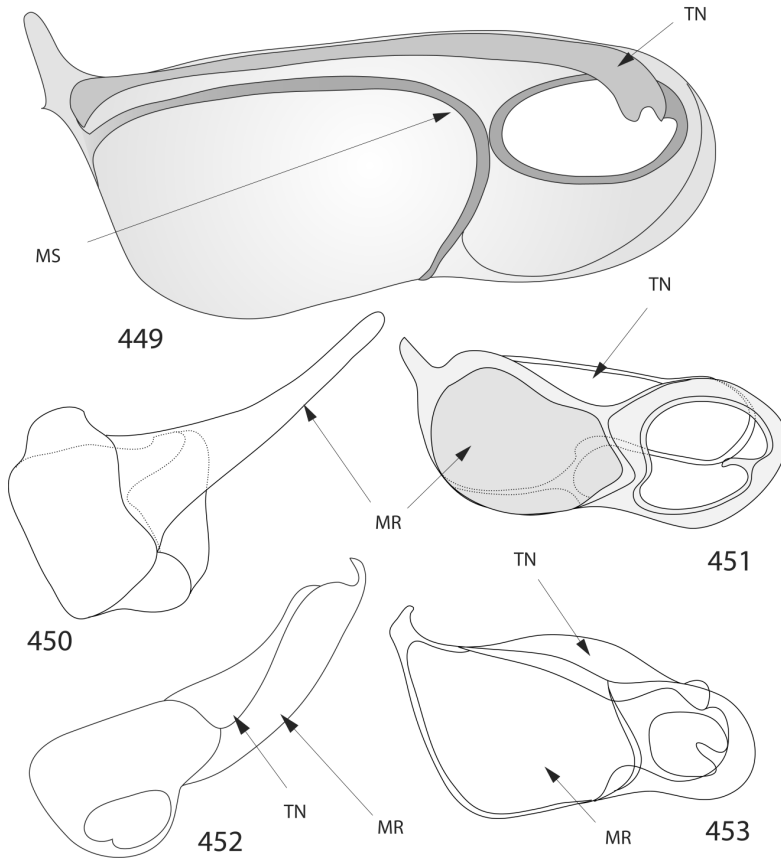
Figs 449-453: Metacoxae: *Dexoris tessmani* Bocák & Bocáková, metacoxa, internal view (449); *Dilophotes depressicornis* Pic, metacoxa, dorsal view (450); same, internal view (451); *Mesolycus shelfordi* (Bourgeois), metacoxa, ventral view (452); same, internal view (453).

MR -meron; MS - meral suture; TN - trochantin.

The radial bar is formed by more or less developed C, Sc and RA veins, Sc usually forked near the wing base, with its posterior branch fused to RA near the middle of the costa (e.g. *Dilophotes*, Fig. 402). In a number of taxa, however, i.e. *Conderis* and *Proteros*, Sc separate from RA after having joined or slightly touched it and merge with C not far from the apical hinge (Figs 406, 413). In *Dexoris* all of PC+C, Sc and RA run parallel before entering the flattened bar distad of the middle of the costa (Fig. 398). In rare instances the PC vein seems to be manifest at the base of the wing (i.e. *Eropterus*, Fig. 414). In *Alyculus* and *Phengodes* the RA vein almost attains to the apex of the wing (Figs 419, 421).

The radial cell is well developed, from somewhat transverse (e.g. *Miniduliticola*, Fig. 409) to conspicuously elongate (e.g. *Caenia*, Fig. 407). Sometimes two radial cells are present, as in *Dexoris* and *Lycostomus* (Figs 394, 398); in what seems to be the extreme case there are three radial cells (*Lampyrolycus*, Fig. 401). The RAr vein is reduced in majority of lycids, being more or less developed only in the
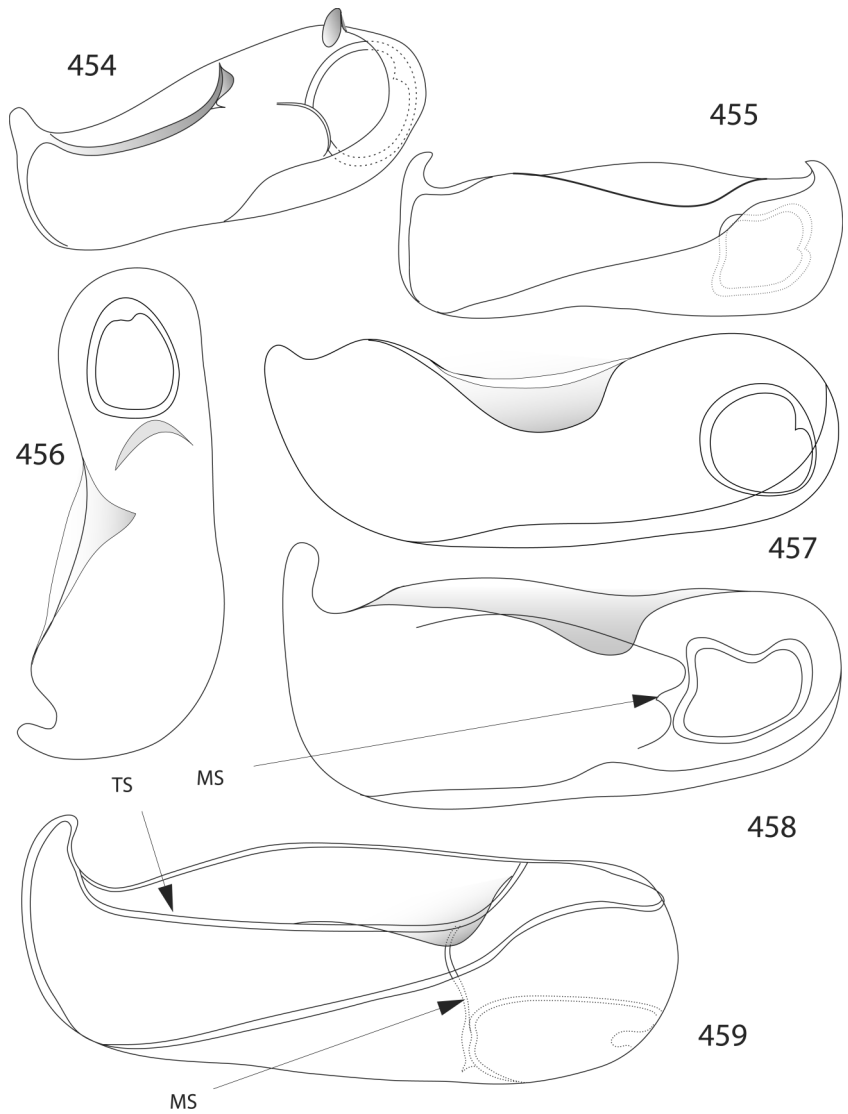
Figs 454-459: Metacoxae, internal view: *Caenia kirschi* Bourgeois (454); *Lyroneces optabilis* (Kleine) (455); *Scarelus umbrosus* Kleine (456); *Platerodrilus* sp. (457); *Ceratoprion* sp. (458); *Calopteron reticulatum* (Fabricius) (459).

MS - meral suture; TS - trochantinal suture.

apical part of the wing where it usually takes part in forming the radial cell(s) (Figs 394-418).

The apical field of the hind wing has typically two or more vague sclerotizations or pigment patches, the anterior, obviously homologous with the pterostigma, sometimes forming a vein-like structure, as in *Miniduliticola* and *Thilmanus* and to some extent in *Dexoris* (Figs 398, 409, 420), and the posterior patch generally
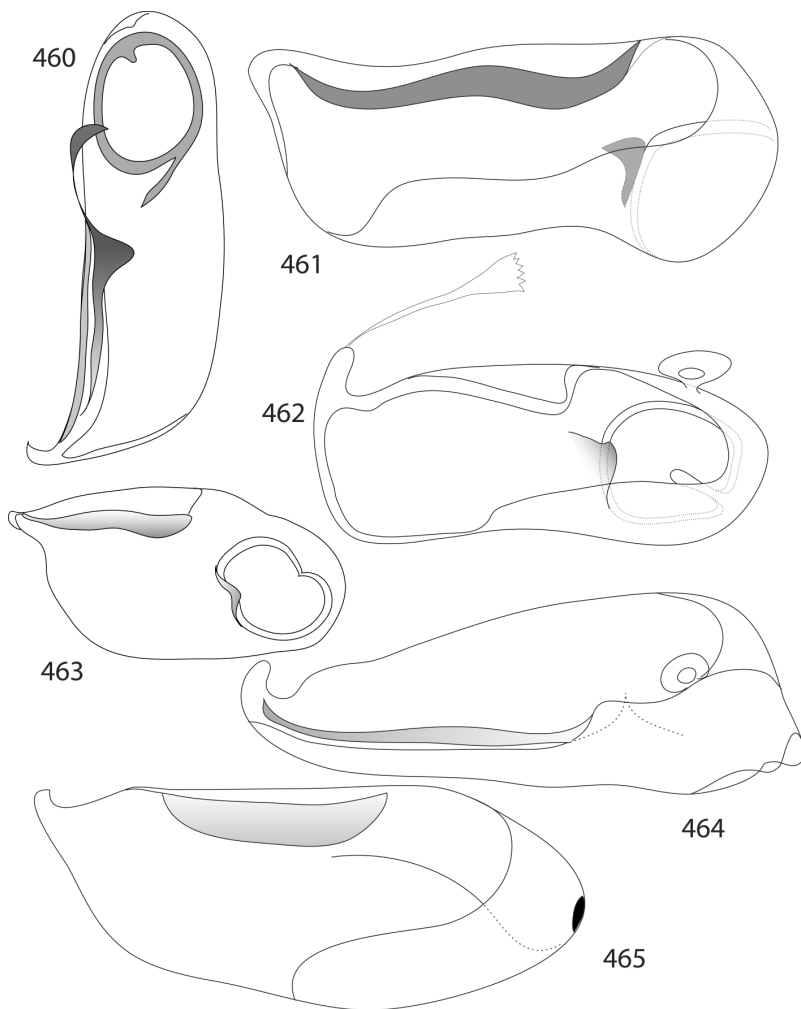
Figs 460-465: Metacoxae, internal view: *Plateros flavoscutellatus* Blatchley (460); *Macrolycus flabellatus* (Motschulsky) (461); *Lycostomus praeustus* (Fabricius) (462); *Metriorrhynchus thoracicus* (Fabricius) (463); *Lampyris* sp. (464); *Phengodes* sp. (465).

remaining obscure. *Phengodes*, on the other hand, has noticeable, though somewhat feeble, but equally developed anterior and posterior vein-like patches (Fig. 421).

The RP vein is often short, but attaining to the wing base and the RA vein in *Lycostomus* (Fig. 394), being nearly so in *Dexoris*, *Scarelus*, *Caenia*, *Metriorrhynchus*, almost all Erotinae and some others (Figs 398, 400, 407, 411, 413-415, etc.).

The Cu vein is typically merged to M, but in some cases (*Lyroneces*, *Autaphes*, *Ceratoprion*, Figs 395, 397, 412) is not, being more or less prolonged basally. The only taxon where the Cu vein seems to be merged to the anal veins is *Miniduliticola* (Fig. 409). The merger of Cu with M or A veins was probably caused by the strong longitudinal fold transecting it basally. The basal persistence of the suppressed Cu
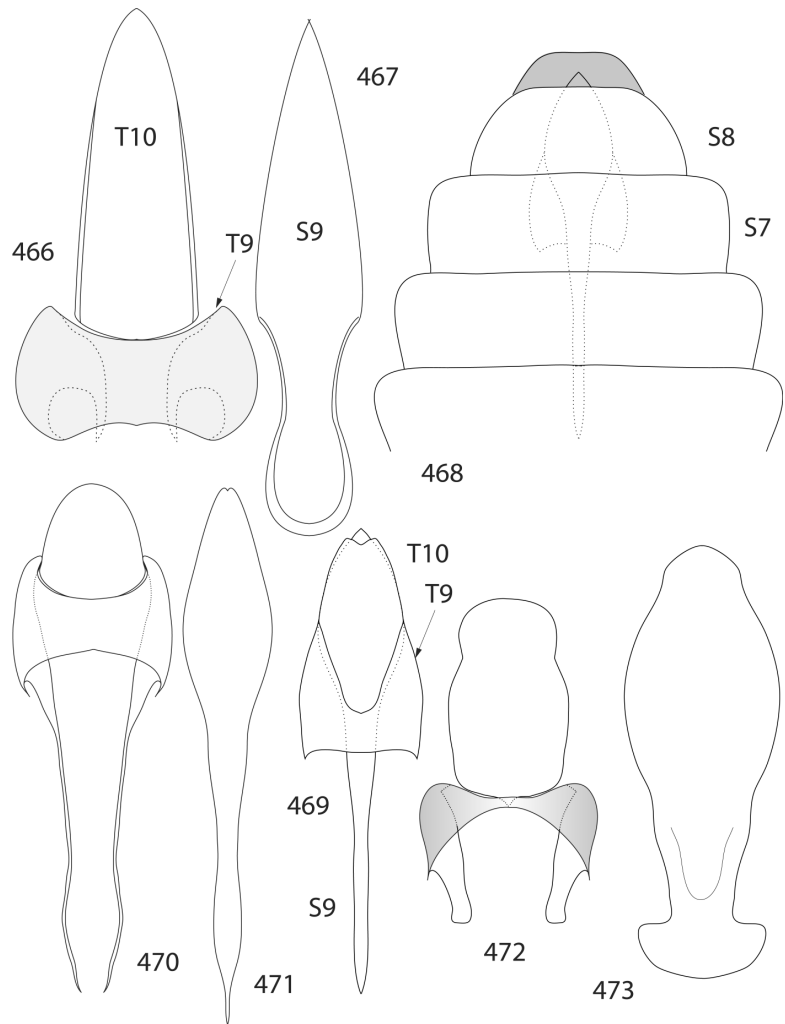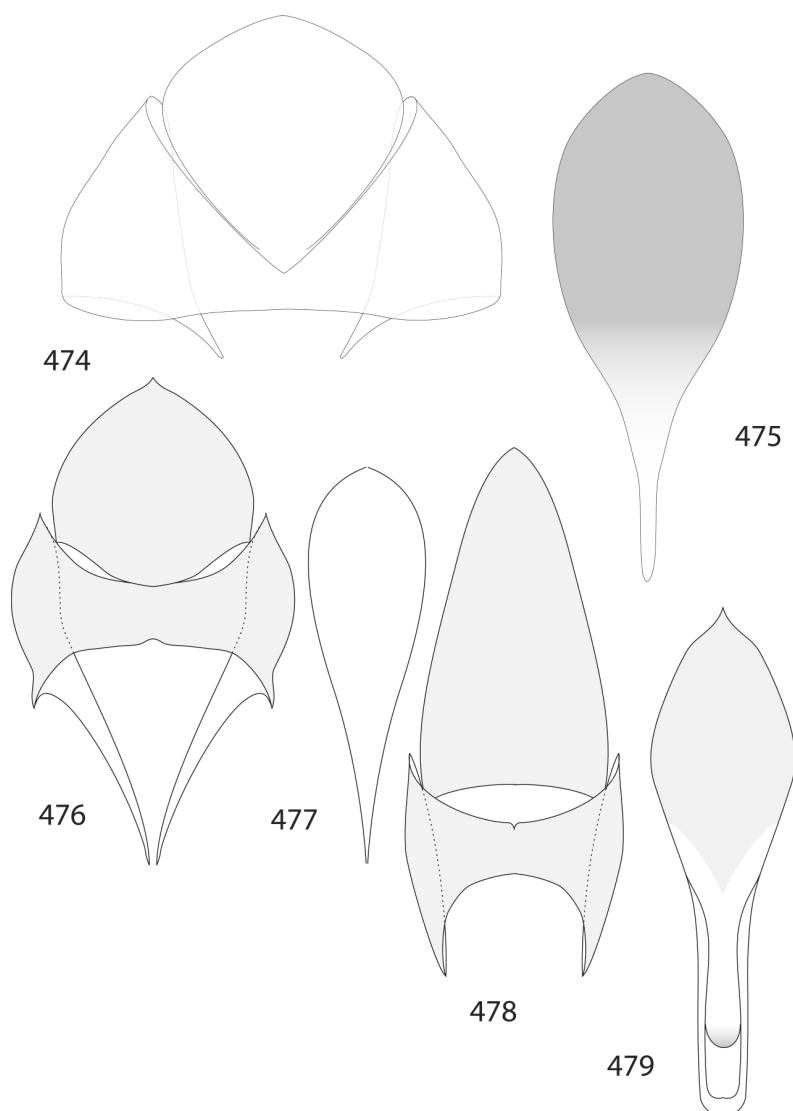
Figs 466-473: Imaginal terminal male abdominal segments: *Lycostomus praeustus* (Fabricius), tergites, dorsal view (466); same, ventrite, ventral view (467); *Flagrax auberti* (Bourgeois), ventrites 5 to 7, showing retracted apical segment, ventral view (468); same, retracted tergites, dorsal view (469); *Proteros sempiternus* Kazantsev, tergites, dorsal view (470), same, ventrite, ventral view (471); *Macrolycus flabellatus* (Motschulsky), tergites, dorsal view (472), same, ventrite, ventral view (473).

S - sternite; T - tergite.

vein, which is typically fused to 1A (Fig. 393), seems to agree with this hypothesis. In *Thilmanus* the Cu vein is suppressed altogether (Fig. 420).

The anal cell is always closed in the lycid hind wing, the only exception being *Alyculus* (Fig. 419). The anal cell sometimes appears to be closed with a transverse brace (*Lycostomus*, *Dexoris*, *Ceratoprion*, *Scarelus*, *Conderis*, Figs 394, 397, 398, 400, 406, etc.). The closed wedge cell is characteristic of Erotinae, as well as *Lampyrolycus*, *Broxylus* and *Dilophotes* (Figs 401, 413-418), while its absence is a

Figs 474-479: Imaginal terminal male abdominal segments: *Dexoris tessmani* Bocák & Bocáková, tergites, dorsal view (474); same, ventrite, ventral view (475); *Scarelus umbrosus* Kleine, tergites, dorsal view (476); same, ventrite, ventral view (477); *Platerodrilus* sp., tergites, dorsal view (478), same, ventrite, ventral view (479).

more widespread condition in the family (Figs 394-400, 402-412), as well as in Lampyridae and Cantharidae (Brancucci, 1980).

The cubital and anal groups of veins are typically connected with each other by cu-a transverse brace (e.g. Figs 400-402, 410-412, etc.). The relatively few taxa that do not have the cu-a connection include *Ceratoprion*, *Macrolycus*, *Mesolycus*, *Lyroneces* and *Platerodrilus* (Figs 395, 397, 404, 405, 403). The cu-a brace is